Hindawi
Advances in Civil Engineering
Volume 2019, Article ID 6585102, 14 pages
https://doi.org/10.1155/2019/6585102

Research Article

A Multistory Building Evacuation Model Based on Multiple-Factor Analysis

Yang Zhou, Tanghong Wu, Gaofan Zhang, and Zichuan Fan

School of Computer and Information Science, Southwest University, 400715 Chongqing, China

Correspondence should be addressed to Zichuan Fan; fanzc@swu.edu.cn

Received 11 March 2019; Revised 8 April 2019; Accepted 11 April 2019; Published 2 June 2019

Academic Editor: Hayri Baytan Ozmen

Emergency evacuation is an important issue in public security. To make a considerate plan, various situations are presented including blocking the accident area and letting the emergency access path available. In order to offer dynamic evacuation routes due to different circumstances, a multistory building evacuation model is proposed. Firstly, to analyse the patency of the building, an evacuation formula is applied after binary processing. The function of evacuation time and some other parameters is given by means of regression analysis. Secondly, the cellular automata (CA) algorithm was applied to illustrate the effect of the bottleneck. The response of evacuation time could be approximately optimized through calculating time step of the CA simulation. Finally, the value of maximum evacuation population density could be determined according to the analysis of CA simulation results, which was related to the switch state of the emergency channel. The emergency evacuation model was simulated by using the Louvre museum as an example. The results of the simulation presented some feasible evacuation routes in all kinds of situations. Furthermore, the functional relationship would also be given among evacuation time with the diversity of tourists, pedestrian density, and width of exits. It can give a different perspective that the multistory building evacuation model shows excellent adaptability to different circumstances.

1. Introduction

In recent years, there have been many terrorist attacks around the world, which poses a great threat to the safety of residents and tourists [1, 2] and caused great psychological trauma to the victims after terrorist attacks [3, 4]. Terrorist attacks require the rapid evacuation of all tourists. The safety of tourists, evacuation time, and emergency handling are always the focus of such problem.

This paper would discuss the evacuation of multistory buildings based on the Louvre terrorist attack [5, 6]. To measure the number of people and to detect an emergency condition in the building, two devices have been included in Louvre's evacuation system. Preprocessing of binary images can describe the details of Louvre's architectural thoroughly. The location of the bottleneck can be determined by analysing the patency rate. Furthermore, the multistory building evacuation algorithm was established to provide dynamic optimal path allocation, where the emergency and dangerous area were considered based on the 3D model. A cellular automata (CA) model was used to simulate the effect of the bottleneck on evacuation time and modified the evacuation time [7]. It is necessary to simulate the situations of congestion in the accident area and allow the emergency personnel to enter the Louvre. According to the simulation data, the influence of diversity of tourists (disability, age group, and pregnant women), pedestrian density, and width of exits on evacuation time was analysed. It should be pointed out that the adaptation of the model in different buildings may be verified by the simulation of evacuation in rectangular, L-shaped, and composite structures.

In this paper, the summary and unnoticed things of related work were studied and discussed in Section 2. Image processing and evaluation formula of the patency of the bottleneck were discussed and calculated in Section 2. Moreover, a multistory building evacuation algorithm was used to calculate the optimal path, and the cellular automata

model was used to simulate. Section 3 simulated the evacuation routes planning for different emergency situations. Section 4 analysed the influence of different variables on evacuation time based on the simulation data. Finally, the conclusions were shown in Section 5.

2. Related Works

The evacuation system in the building has been a hot issue over recent decades [8, 9], especially for multifloor building with at least one certain stairway or elevator. Different methods such as cellular automata models, social force models, and fluid-dynamic models have been investigated based on mathematics by computing.

Early works proposed a classic problem which is a highly transient, stochastic, nonlinear, integer programming problem [10]. A utilizing queueing network model was proved useful in the design of emergency evacuation plans soon after. Targeting at these issues, Pauls [11] summarized the history of investigations into calculating evacuation times, including the basic concepts along with selected calculation methods [11]. Moreover, Smith [10] discussed this special class of problem. His team improved the previous methodology by adding state-dependent queueing models to capture the nonlinear effects of increased occupant traffic flow along emergency evacuation routes [10].

A preliminary model was proposed by Liu et al. [12] in 2009. In the context of evacuation from a water-related hazard, his team prototyped a multiagent-based evacuation simulation system. But relevant work is short for the definition of evacuation congestion in the numerical value. The functional relationship between evacuation time and correlation factors should also be investigated deeper. Furthermore, the arrangement of emergency personnel entering the building and dangerous situations and their safety should be considered in some special circumstances.

Ma et al. [13] proposed an ultrahigh-rise building evacuation model with elevator aided based on cellular automaton which considered pedestrian movement and elevator operation. After summarizing previous researches, flow capacity and human behavior were considered to be of great importance in investigating the safety of the evacuation process. During the same period, Zhang et al. [14] established a multinode hierarchical data model based on a hierarchical route algorithm. A large crowd evacuation simulation was then given. They also gave some social factors to the model as the formula of social force. Their 3D model showed more efficiently on the topological relations and geometric properties of the building features. However, such previous research has not considered the influence brought by the diversity of tourists. In addition, the evacuation time and related factors may not be accurate with the calculation of the evacuation route.

Xiong et al. [15] proposed a dynamic indoor field model with three typical characteristics. Firstly, there was not only static information but also dynamic information, such as outdoor and indoor building geometry, sensors, fire spread, and personal behavior. Spatial calculations were given based on a three-dimensional space grid. They analysed potential congestion and stagnation during the evacuation. The result of the designed evacuation method can support individual evacuation route and evacuation assessment.

3. Model Design

3.1. Image Preprocessing. An accurate evacuation plan needs a schematic diagram of the floor plan, which thoroughly described the architectural details of Louvre. It is reasonable to put the structure map of Louvre into binarization as a pretreatment after analysing the map [16]. The gray level image of the Louvre area should be converted into a binary image based on im2bw function of Matlab [17]. To realize the binarization of the map, the grayscale of pixels which is larger than a certain gray value should be set as 1; similarly, the gray level which is less than this value should be set as the 0. Hence, the quantifying terrain factor was accomplished. Figure 1 shows the result of the binarization of the ground floor in the exhibition area.

3.2. Bottleneck Location Determination Model. When an emergency situation happened, exits would be filled with evacuees immediately. The number of people in each exit of the exhibition area will increase sharply due to the panic sensation of the visitors. Visitors will peak the human density at the exit which exceeds the maximum operational capacity. Such disturbance will finally result in congestion. This kind of phenomenon, which limited people's activity space, is defined as the bottleneck in this paper. As the maximum allowable pedestrian movement is not enough for evacuation flow of the exit, a semiellipse-shaped crowded area will appear at the exit. Hence, this paper investigated the extent of bottlenecks by examining the characteristics of the semiellipse area.

As shown in Figure 2, the yellow part represents the exit. The white area means the tendency of export population evacuation where the individual in a group of people is simplified into a single white point. The red semiellipse border shows a standard trend of the congestion area. The exit is simplified into a two-dimensional rectangular space of length l and height h, with the midpoint of the exit as the origin. Due to the complicated and narrow terrain of the Louvre, the increasing human density at the exits is also restricted by the topography inside, which is also one of the key factors causing the bottleneck.

The bottleneck is a dynamic process which starts from generation to enlargement and then disappearance. The approximate semielliptical shadow area near the exit in Figure 2 indicates the area of bottleneck S. The discriminant equations of bottleneck B_{ott} are as follows:

$$B_{\text{ott}} \begin{cases} S = 2\int_0^p \frac{q}{p}\sqrt{p^2 - x^2}\,dx, \\ S_0 = hl, \\ r = \frac{S}{S_0}, \end{cases} \tag{1}$$

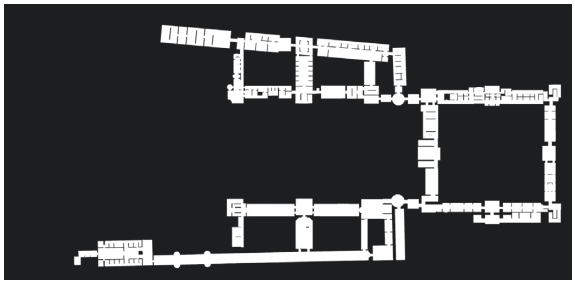

Figure 1: The binarization of topographic distribution on the first floor of the Louvre.

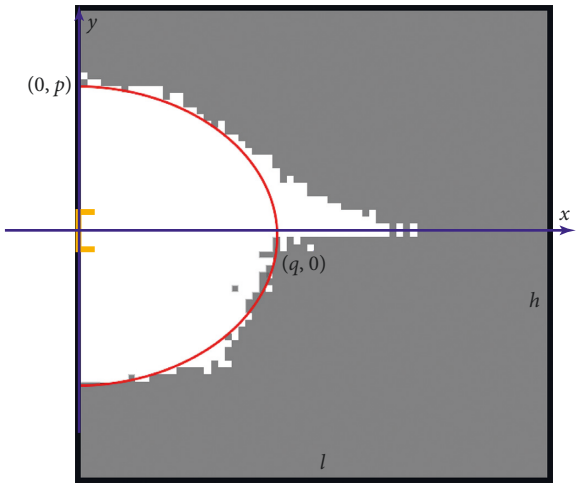

Figure 2: An illustrative diagram of the bottleneck.

where p is the short semiaxis length of the ellipse, q is the long semiaxis length of the semiellipse, S is the area of semiellipse, S_0 is the area of the rectangular space, and R is the ratio between S and S_0. This paper regulated that the bottleneck occurs when elliptical area S occupies 10% of the space area S_0. To ensure personal safety, the proportion of the certain area in the model should be less than 30%.

In terms of the patency rate, after obtaining the binary matrix of Louvre's topographic distribution, all the possible bottlenecks in the certain floor were analysed on the basis of the binary graph. Consequently, the O_{bs} evaluation formula of patency was applied in the model according to the interaction among points in the k-means clustering algorithm.

As for the index of the similarity degree, individual with larger correlation coefficient "C_a" has more similarity. In the planar structure of the Louvre, the coefficient of the movable range (white region) which is signed as 1 has an influence on other people, while the coefficient of inaccessible range (black region) which is signed as 0 has no influence on other people. The smaller the distance index O_d is, the more similar it is for individuals.

Euclidean distance was used as the evaluation index in terms of the planar structure of the Louvre in this paper. Exponential attenuation function can establish the discriminant function based on the Euclidean distance. The exponential function (base e) was chosen as the correlation discriminant function. The O_{bs} evaluation formula of the patency is shown as follows [18].

$$O_{bs} = f(O_d) = \sum_{n=1}^{\infty} A_0 e^{-O_d \times b + c},$$
$$O_d = \sqrt{(x_n - x)^2 + (y_n - y)^2}, \tag{2}$$

where $(x,\ y)$ is the coordinate position of the point to be evaluated, (x_n, y_n) is the coordinate position of some other point, A_0 is the amplitude of the evaluation formula, and b and c are variables related to the sensitivity of the discriminant function.

Then, the evaluation system was applied to the binary matrix of the Louvre terrain distribution which obtained the patency coefficient of each point in the matrix. The distribution is shown in Figure 3.

The channel may be congested, as shown in Figure 3. Patency rate of the region could be seen by the corresponding value of the ribbon. The blue area represents inaccessible, the green part represents congested, and the yellow part represents smooth.

If turning the image into 3D, congestion would be more likely to occur when the contribution rate was lower. The potential point of the bottleneck signed as "×" at the valley is indicated in Figure 4 ($D1, \ldots, D5$ represents 5 regional distribution of Louvre in hereinafter).

3.3. Multistory Building Evacuation Algorithm. The Louvre is a multistory building. The model building and algorithm design are quite different compared to single-story buildings. There must be some common parts due to the limited path capacity and common areas among floors. Higher source points need to share certain sections with lower source points. The actual flow of these shared sections is generally affected by the convergence of staff on each floor. Hence, the pedestrian movement "n" in each path is not always a constant but a variable that changed constantly according to time.

Before construction, the rules for the multistory building evacuation algorithm were defined as follows [17]:

Rule 1: if $P_1, P_2, \ldots, P_k$ is the path selected to evacuating people, then all evacuation groups in the optimal evacuation plan require an equal evacuation time, which is indicated as $T_1, T_2, \ldots, T_k$

Rule 2: let P be an aggregation of paths determined by the feasible path algorithm. For any path $P_k \in P$, adding the path P_k to the set of feasible paths will not improve the evacuation scheme

Rule 3: let P be a set of feasible paths determined by subalgorithms. For the elements of P satisfying $T_1 \le T_2 \le \ldots \le T_k$, the optimal evacuation routes $P_1, P_2, \ldots, P_k$ $(m_1 \le m)$ are determined by

$$\sum_{k=1}^{m_1} \left(T_{p_{m_1}} - \left(T_{p_k} - 1\right)\right) f_k \le x \le \sum_{k=1}^{m_1+1} \left(T_{p_{m_1+1}} - \left(T_{p_k} - 1\right)\right) f_k. \tag{3}$$

In order to optimize the whole evacuation model of Louvre, the minimization of evacuation time was taken as

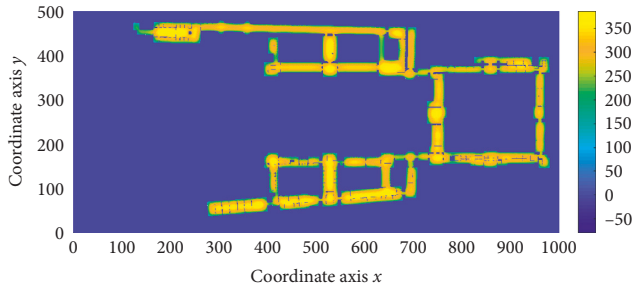

Figure 3: Patency distribution map of each area on the first floor of the Louvre.

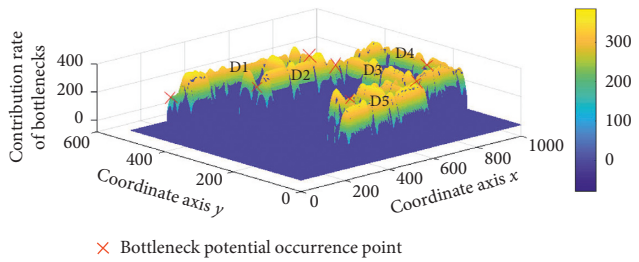

Figure 4: 3D diagram of regional patency on the first floor of the Louvre.

the objective function. Considering the existence of the common section, the floor requiring longer evacuation time should be evacuated first. Meanwhile, the shorter evacuation route should be saturated to optimize utilization of time.

The following is a partial description of the algorithm for the evacuation model of multistory buildings [13]:

Step 0: initialize the input floor set S. Initialize the number of people who need to be evacuated on each floor; initialize the passage time t_{ij} of each section; initialize the total number of trapped people in each layer input q^{W}; add Z_0 as the superoutlet, Z_0 is the set of four exits in the Louvre which is signed as C_2, C_5, C_7, and E_1 in the following text; $K_0^{W_r}$ is the initial evacuation route set; H is the floor set; F is the dynamic flow set; Γ is the evacuation time set of each floor.

Step 1: use Dijkstra algorithm to find the shortest path P_w from evacuation zone S to superterminal Z_0 and calculate the passage time T_{P_w} of the path.

Step 2: calculate the maximum capacity P_k of the path. Let $f_k = \min\{c_{ij} \mid e_{ij} \in P_k\}$, and update the maximum capacity:

$$c_{ij} = \begin{cases} c_{ij} - f_k, & e_{ij} \subseteq p_k, \\ c_{ij}, & e_{ij} \subsetneq p_k, \end{cases} \tag{4}$$

on each arc. If $c_{ij} = 0$, delete the arc e_{ij} from the original network and update the network.

Step 3: determine the path set $K_{w_r \cup k,r}\{P_k^{W_r}\}$ for evacuation according to $\{P_1, P_2, \ldots, P_{mi}\}$, end of evacuation time $\Gamma_0 = \cup\{T_{w_r}\}$, and traffic collection $F_0 = \{f_k^{W_r}\}$. The flow chart of the algorithm is shown in Figure 5.

3.4. Cellular Automata Model. In actual situations, the number of evacuees in the Louvre is possible to be greater than the sum of the maximum capacity per unit time of all paths [19]. Hence, during the process of evacuation, people rushing into exits can result in different degrees of bottlenecks, which greatly extended the evacuation time of each section of the road. Due to this situation, the evacuation time Γ of each path calculated through the multistory building evacuation model (model 2) was not accurate and meaningless.

To solve the problem, modifying the evacuation time aggregation Γ of each layer through the CA model must be done to simulate the effect of the bottleneck on evacuation time, which means to infer the revised evacuation time aggregation Γ^* of each layer [20]. As a common method, the dynamic process of crowd evacuation can be observed intuitively using the cellular automata model. It also helps to discuss the determinants of bottlenecks. Therefore, this paper modifies and simulates the agent model through cellular automata.

Regarded as a dynamic system in a cellular space, CA is composed of discrete, finite state cells. CA evolves in discrete time dimension according to certain local rules. Each cell has one or more states as a specific parameter. The state of the cell was selected in the finite state set such as the spatial characteristic "occupied and vacant." In the cellular automata model, the evacuation pedestrian can only move the length of one cell within each time step t. Two dynamic parameter values including the direction parameter and the space parameter is the sum of the mobile income. Its formula is represented as follows:

$$P_{ij} = D_{ij} + E_{ij}, \tag{5}$$

where P_{ij} is the mobile income parameter, D_{ij} is the directional dynamic parameter, and E_{ij} is the space dynamic parameter. The simulation process using cellular automata is shown in Figure 6.

Some significant parameters will be explained in the following sections.

3.4.1. Description of Competitiveness Value. Due to the difference of age and physical fitness of individual based on the cellular automata model, the competitiveness value C_{omp} is put forward to describe the ability of the agent reaching the target point firstly when encountering a conflict of the target point. The bigger the value of the individual's competitiveness is, the easier it is to win the confliction and reach the target point.

Taking into consideration that personal physiological aspects have gender G_{en}, age A_{ge}, the degree of disability D_{is}, and whether to bring a child C_{hi}, the competitiveness formula is represented as follows:

$$C_{omp} \begin{cases} \dfrac{G_{en} + (A_{ge}/18) - C_{hi}}{D_{is}}, & 0 \le A_{ge} \le 22, \\ \dfrac{G_{en} + (40/A_{ge}) - C_{hi}}{D_{is}}, & 22 < A_{ge}. \end{cases} \tag{6}$$

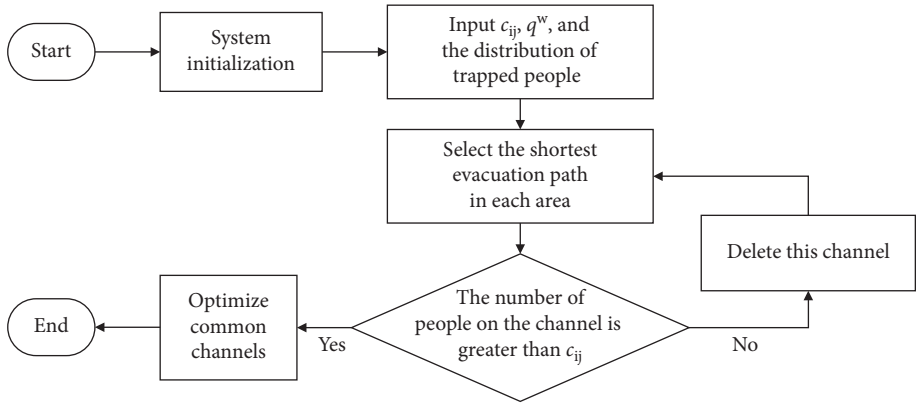

Figure 5: Algorithm flow chart of model two.

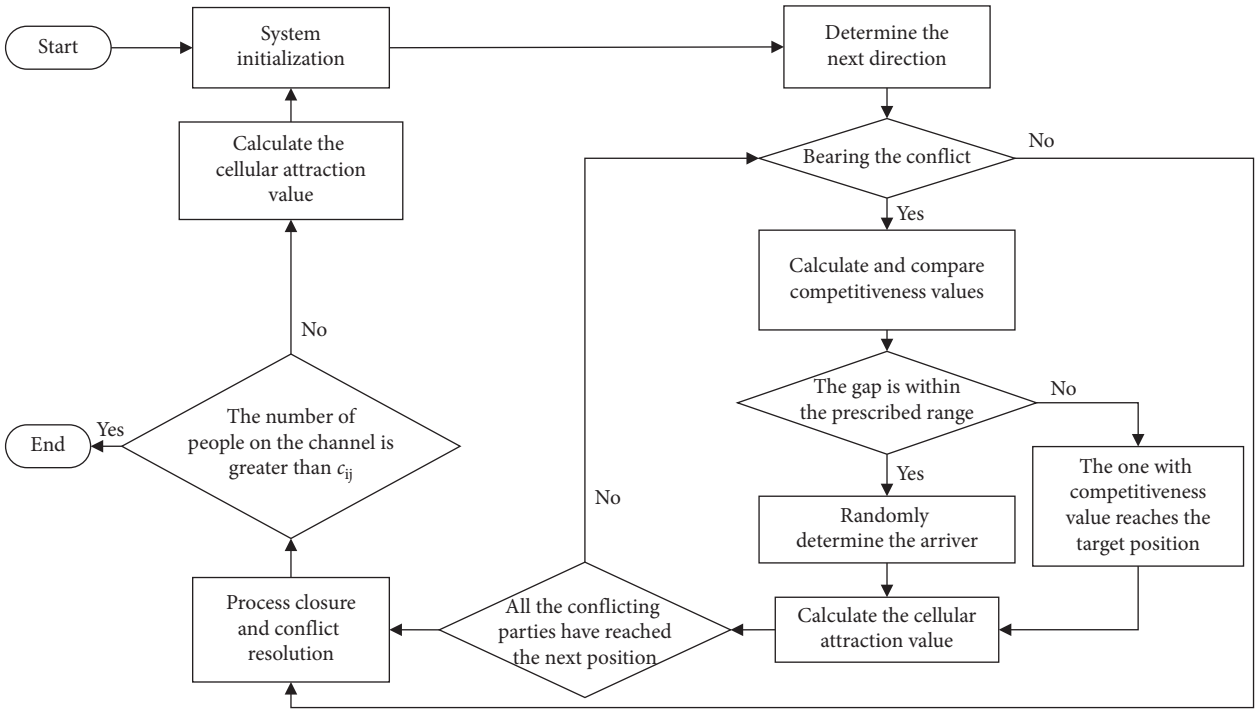

Figure 6: Simulation flow chart based on CA.

3.4.2. Cell. The simulation model of pedestrian evacuation is built in a 2D discrete cellular grid system with the size of $U_x \times U_y$. The moving area of pedestrian evacuation space was divided into $U_x \times U_y$ discrete cellular spaces with equal size. There is only one pedestrian that can be accommodated in each cell position in the system. The pedestrian simulation process is also discretized to equal time step. Within each discrete time step, a pedestrian can only move a cell's position.

3.4.3. Directional Dynamic Parameter. In a moving area where evacuees are located in the center, the value of the corresponding directional parameter matrix element is shown as follows:

$$D_{ij} = \begin{cases} \dfrac{S_{00} - S_{ij}}{1}, & i + j = 1 \text{ or } -1, \\ \dfrac{S_{00} - S_{ij}}{\sqrt{2}}, & i + j = 1, 2, \text{ or } -2, \end{cases} \tag{7}$$

where S_{00} is the shortest distance of the safe exit in the center of the mobile field and S_{ij} is the shortest distance from cellular (i, j) to safe exit in pedestrian movement field.

3.4.4. Space Dynamic Parameter. Pedestrians are not allowed to cross fences or obstacles; at the same time, they can get out of the cellular space only through the safe exit of the room. The value of the center cellular position is 0. If the

cell is not occupied by a person or an obstacle, its occupation value is 1; otherwise, is −1. If the cell is −1, pedestrians in the center cell cannot reach this cell:

$$E_{ij} = \begin{cases} 1, & \text{empty cellular,} \\ 0, & \text{central cellular,} \\ 1, & \text{central occupied or obstructed.} \end{cases} \quad (8)$$

3.4.5. Attraction. Attraction S is used to describe the behavior of pedestrians which tend to choose the nearest exit. Pedestrian evacuation movement is purposeful and directional. The destination of pedestrian evacuation is the exit. The direction of movement is the safe direction of the pedestrian evacuation. The closer the cellular position is to the exit, the stronger the attraction of the cell is to the pedestrian, and the bigger the possibility is to the pedestrian entering the exit. The formula for calculating the attraction of a cell is as follows [7, 21]:

$$S_{ij} = \begin{cases} \dfrac{1}{\min_m\left(\sqrt{\left(x - x_n^m\right)^2 + \left(y - y_n^m\right)^2}\right)}, & \text{empty cellular,} \\ M, & \text{cellular with obstacles,} \end{cases} \quad (9)$$

where S_{xy} is the shortest distance from the cellular (x, y) to the safe exit, (x, y) are coordinates of cells in the evacuation system, (x_n^m, y_n^m) are coordinates in the evacuation system of the n^{th} cell from m^{th} room, and M is a positive number which tends to infinity. The plan of the simplified refuge floor and the corresponding static floor field for the doors with the colour bar indicate different distant values, as shown in Figure 7. The red part indicates the exits whose center points are (40, 0) and (60, 0) and (30, 0), (70, 0), and (50, 100), respectively. The contour line indicates the attraction of individual. The darker the colour is, the less attractive it is for each person.

In Figure 8, simulation by using cellular automata method gives three different conditions during evacuation. Figure 8(a) shows a state of an impending bottleneck, Figure 8(b) shows the state of the bottleneck when it reaches a critical size, and Figure 8(c) shows a state in the bottleneck recession.

4. Simulated Analysis of Multistory Building Evacuation Algorithm

4.1. Simulation of Emergency Evacuation. Based on the multistory building evacuation model established in the previous sections, the model area partition and connection channel were shown in the schematic diagram (Figure 9). The dots of each layer in the 3D diagram represent regions, and the line segments represent the channels [14]. The evacuation algorithm for the multistory buildings was simulated and programmed based on Matlab and presented on the 3D model [18].

Each floor of the Louvre is divided into areas depending on where the bottleneck may occur [14]. Figure 9 shows the ideal plan of the leaving Louvre after transformation. The triangles represent four exits, different colours represent the area of different floors (or the exit of the layer), and each line represents the passage or stairway among each area; the value was obtained according to the distance of each channel. Four points, $A3$, $A6$, $B4$, and $B7$, were selected to simulate the evacuation points of the people. Then, the certain number of evacuees was simulated in each of the four districts.

To get the optimal evacuation routes, path capacity and other parameters need to be calculated. Using the algorithm introduced in previous sections, the actual evacuation routes of each floor could be determined. After finding out various solutions of all feasible paths, an optimal evacuation plan can be determined. The simulated results of the evacuation scheme are shown in Table 1.

The evacuation scheme obtained by simulation was expressed by the 3D multistory structure model of the Louvre. As shown in Figure 10, the starting points of the graph are $A3$ and $A6$, where the red part is the routes selected for $A3$ and the blue part is for $A6$. The evacuation paths of each evacuation area were marked with arrows in Figure 10.

Obviously, the capacity of passages was saturated. For example, in the evacuation scheme of the $A3$ region, in the shortest path $A3 \longrightarrow B3 \longrightarrow B4 \longrightarrow C3 \longrightarrow C2$, when the road $A3 \longrightarrow B3$ reaches saturation, it is necessary to reselect $A3 \longrightarrow A7 \longrightarrow B3$ instead of the original scheme.

4.2. Path Planning for Different Emergency Situations. The path scheme would change considering some special circumstances in the museum. There were some different situations discussed: The accident area needs to be sealed off, and evacuees cannot pass through a certain area as the source of fire when the fire occurs; emergency personnel is required to enter the stadium as soon as possible. The simulation design is shown as follows. $A3$ and $A6$ were used as the evacuation point and $B4$ as the accident zone.

4.2.1. Normal Situation. When an emergency would not occur, the initial number of evacuees in $A3$ and $A6$ zones is 600 and 700, respectively. The scheme of evacuation routes is shown in Table 2.

4.2.2. Situation One: Seal the Accident Zone. When the accident happened in zone $B4$, the zone needs to be blocked which means it would not be allowed to enter any more. The scheme of evacuation routes is shown in Table 3.

The evacuation route simulations compare the situation one to the general case by the 3D multistory structure model as shown in Figure 11. Green triangle B4 is the blocked zone. Red triangle $A3$ and blue triangle $A6$ are zones to be evacuated. The red line is the route selection scheme of the evacuation zone $A3$, and the blue line is the route selection scheme of the evacuation zone $A6$.

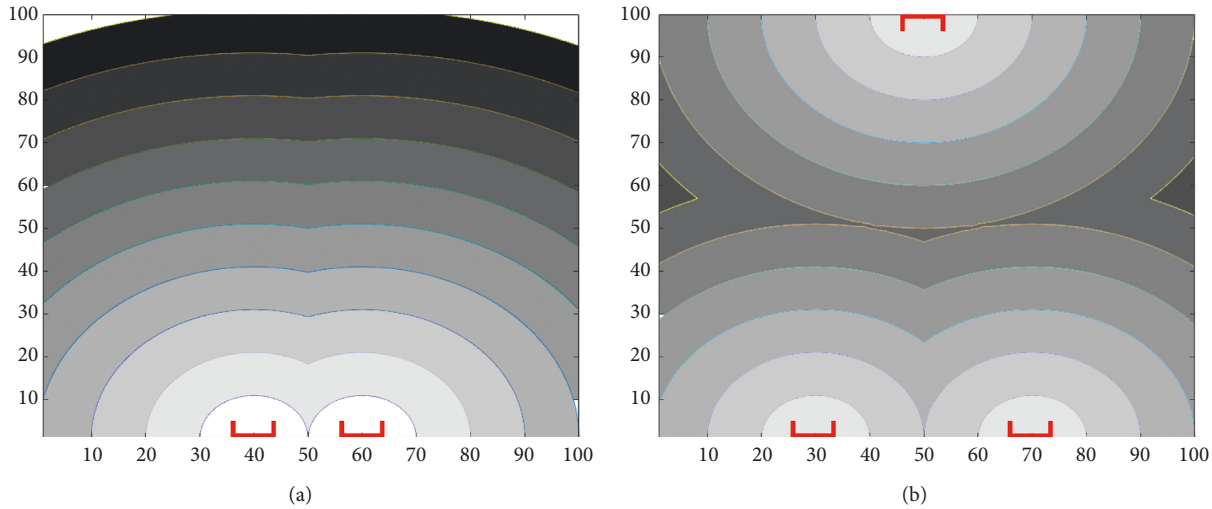

Figure 7: The plan of a static floor field for the doors.

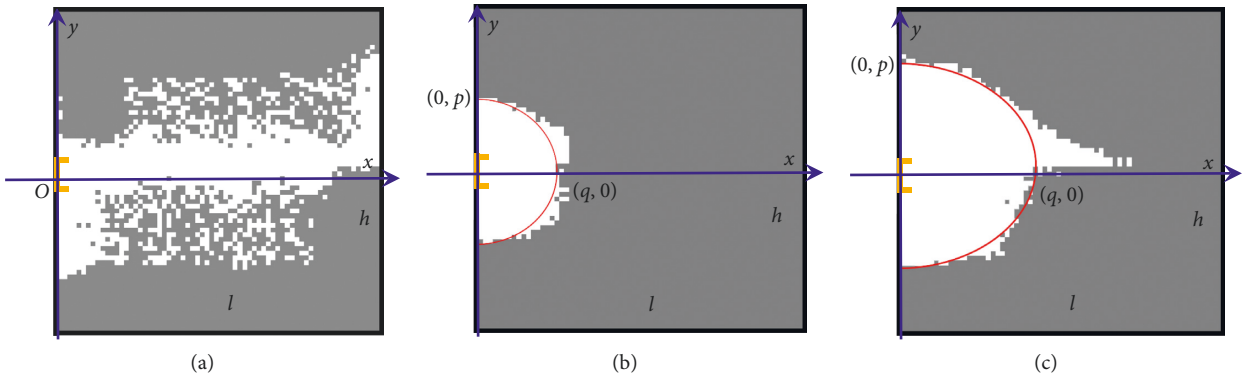

Figure 8: Simulation process of bottleneck formation and disappearance.

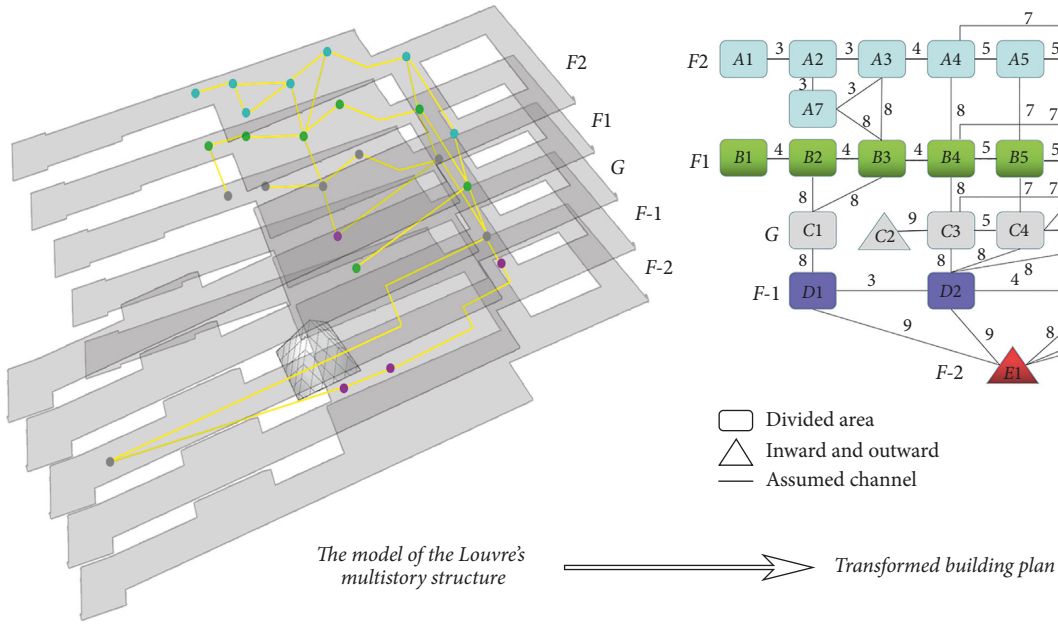

Figure 9: Multilayer structure planarization process diagram of the Louvre.

Table 1: The Louvre evacuation plan table.

Zone	Initial number	Path P	Path length T
Evacuation zone $A3$	600	$A3 \longrightarrow B3 \longrightarrow B4 \longrightarrow C3 \longrightarrow C2$	61.11
		$A3 \longrightarrow A7 \longrightarrow B3 \longrightarrow B4 \longrightarrow C3 \longrightarrow C2$	94.44
Evacuation zone $A6$	700	$A6 \longrightarrow B6 \longrightarrow C4 \longrightarrow D2 \longrightarrow E1$	50.00
		$A6 \longrightarrow A4 \longrightarrow B4 \longrightarrow C3 \longrightarrow C2$	50.00
Evacuation zone $B4$	1000	$B4 \longrightarrow C3 \longrightarrow C2$	23.61
		$B4 \longrightarrow B6 \longrightarrow C4 \longrightarrow D2 \longrightarrow E1$	51.79
		$B4 \longrightarrow B5 \longrightarrow C4 \longrightarrow D2 \longrightarrow E1$	59.29
		$B4 \longrightarrow A4 \longrightarrow A6 \longrightarrow B6 \longrightarrow C4 \longrightarrow D2 \longrightarrow E1$	76.79
Evacuation zone $B7$	800	$B7 \longrightarrow C6 \longrightarrow C5$	25.00
		$B7 \longrightarrow B8 \longrightarrow C7$	29.17
		$B7 \longrightarrow B6 \longrightarrow C4 \longrightarrow C5$	54.17

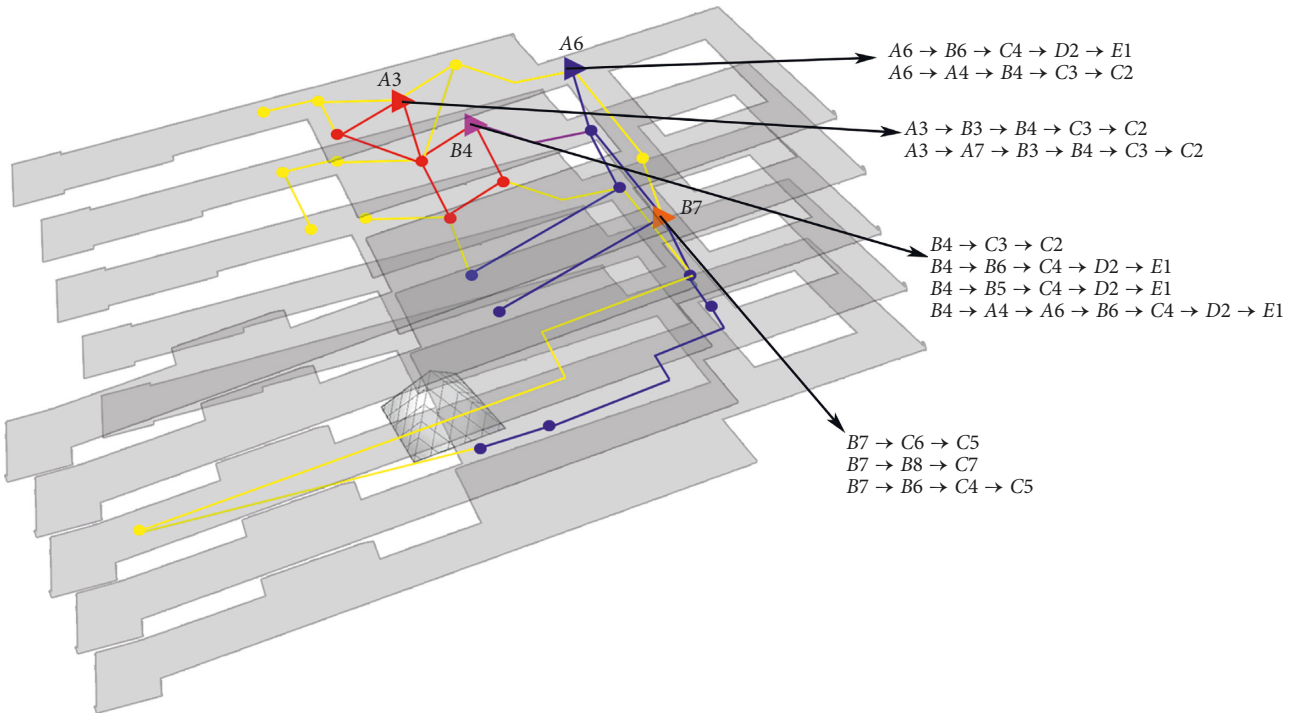

Figure 10: Simulated evacuation scheme.

Table 2: Path planning table in a normal emergency.

Zone	Initial number	Path P	Path length T
Evacuation zone $A3$	600	$A3 \longrightarrow B3 \longrightarrow B4 \longrightarrow C3 \longrightarrow C2$	61.11
		$A3 \longrightarrow A4 \longrightarrow B4 \longrightarrow C3 \longrightarrow C2$	61.11
Evacuation zone $A6$	700	$A6 \longrightarrow B6 \longrightarrow C4 \longrightarrow D2 \longrightarrow E1$	50.00
		$A6 \longrightarrow A4 \longrightarrow B3 \longrightarrow C3 \longrightarrow C2$	50.40

Table 3: The Louvre evacuation plan table.

Zone	Initial number	Path P	Path length T
Evacuation zone $A3$	600	$A3 \longrightarrow B3 \longrightarrow C1 \longrightarrow D5 \longrightarrow E1$	75.00
		$A3 \longrightarrow A4 \longrightarrow A6 \longrightarrow B6 \longrightarrow C4 \longrightarrow D2 \longrightarrow E1$	89.29
		$A3 \longrightarrow A7 \longrightarrow B3 \longrightarrow C1 \longrightarrow D1 \longrightarrow E1$	108.33
Evacuation zone $A6$	700	$A6 \longrightarrow B6 \longrightarrow C4 \longrightarrow D2 \longrightarrow E1$	50.00
		$A6 \longrightarrow A5 \longrightarrow B5 \longrightarrow C4 \longrightarrow D2 \longrightarrow E1$	73.57

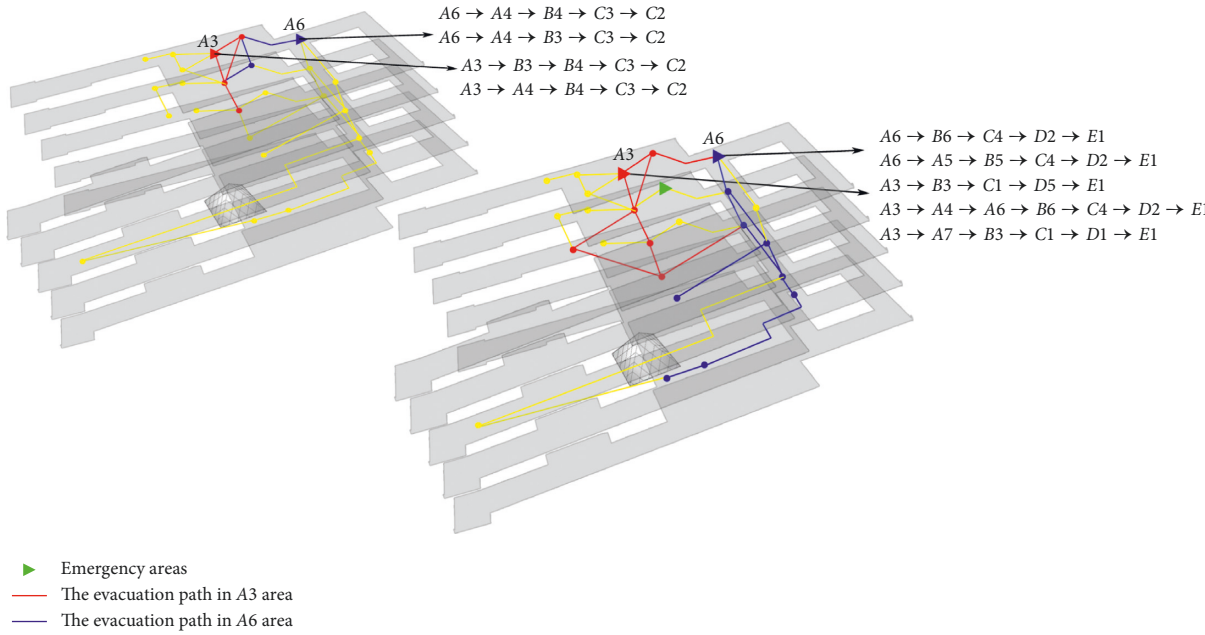

Figure 11: Evacuation route contrast diagram one: evacuation route map of (a) areas $A3$ and $A6$ without a dangerous situation and (b) zones $A3$ and $A6$ when a dangerous situation occurs.

4.2.3. Situation Two: Allowing Emergency Personnel to Enter the Building. When the emergency occurs in $B4$, emergency personnel need to be allowed to enter the area as soon as possible. Emergency access would not be allowed. The scheme of evacuation routes is shown in Table 4.

The evacuation routes simulations results are shown in Figure 12. Green triangle $B4$ is the blockade area, and also the emergency personnel need to reach the point. Red triangle $A3$ and blue triangle $A6$ are areas to be evacuated. The red line is the route selection scheme of the evacuation zone $A3$, and the blue line is the routes selection scheme of the evacuation zone $A6$.

5. Model Optimization and Simulation

5.1. Path Planning for Different Analyses of Topographic Structures. As mentioned above, the Dijkstra algorithm in the multistory building evacuation algorithm could calculate well the length of the shortest path. However, because of the bottleneck caused by congestion, the evacuation time cannot be calculated from the path length directly. Therefore, simulation based on cellular automata is necessary. Then, the functional relationship among evacuation time and other factors was fitted according to the multigroup data further by simulation data analysis.

The program based on Matlab was used to simulate [17]. For the multistory structure model, the crowd dispersion in various regions of the Louvre was simulated, which shows the evacuation situation after calculating the optimal evacuation routes. As shown in the picture, the exhibition area was simulated on the first floor of the Louvre after binarization. The number of cells in the exhibition area was 500×1000, and the number of simulated populations was 10000, which was generated randomly in a movable area. In the simulation diagram, the black area was an inaccessible area such as obstacles or walls. The gray area was an empty cell, and the white parts were cells occupied by a pedestrian (Figure 13).

Through the simulation of cellular automata, the evacuation situation could be observed in a certain area in the multistory building structure model. The simulation of cellular automata could measure and analyse the time of bottleneck occurrence, the area of bottleneck, and time step by giving the planned paths.

In view of the intricate internal structure of the Louvre, the basic topographic structures and simulation results of different populations were discussed in this paper.

5.1.1. Rectangular Spatial Structure. The size of the cellular space is 60×40 rectangular space structure evacuation model, as shown in Figure 14. The number of evacuees was 400, and the people were randomly distributed in the cellular space. The safe exit was located at the center of the wall whose size was 6 units.

Table 5 shows ten times of simulations of evacuation time. Note that the maximum bottleneck areas were under fixed parameters. Through ten times of simulation results, the standard deviation of evacuation time was 13.8076, which showed the range of experimental data was small and the simulation is stable. The average value of the maximum bottleneck area obtained by simulation was 360, as the rectangular region with this parameter tends to result in bottleneck.

5.1.2. Spatial Structure of L-Shaped Channels. The evacuation model of the L-shaped channel spatial structure with the size of 70×100 cells is shown in Figure 15. Simulate when

Table 4: Path planning table in situation two.

Zone	Initial number	Path P	Path length T
Evacuation zone $B4$	0	$E1 \longrightarrow D2 \longrightarrow C4 \longrightarrow B6 \longrightarrow B4$	50.00
Evacuation zone $A3$	600	$A3 \longrightarrow B3 \longrightarrow B4 \longrightarrow C3 \longrightarrow C2$	61.11
		$A3 \longrightarrow A7 \longrightarrow B3 \longrightarrow B4 \longrightarrow C3 \longrightarrow C2$	94.44
		$A3 \longrightarrow A2 \longrightarrow A7 \longrightarrow B3 \longrightarrow B4 \longrightarrow C3 \longrightarrow C2$	127.78
Evacuation zone $A6$	700	$A6 \longrightarrow A4 \longrightarrow B4 \longrightarrow C3 \longrightarrow C2$	50.00
		$A6 \longrightarrow A4 \longrightarrow B3 \longrightarrow C3 \longrightarrow C2$	50.40

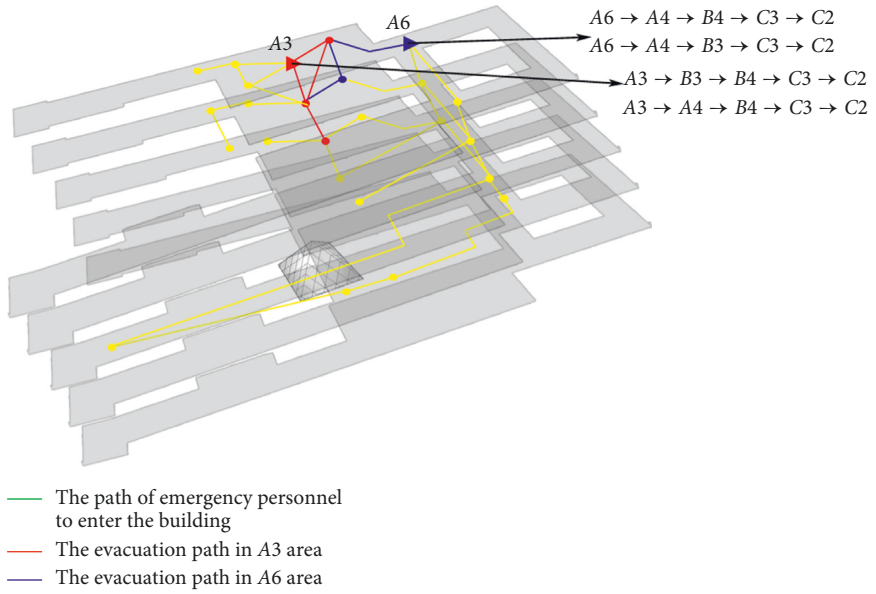

(a)

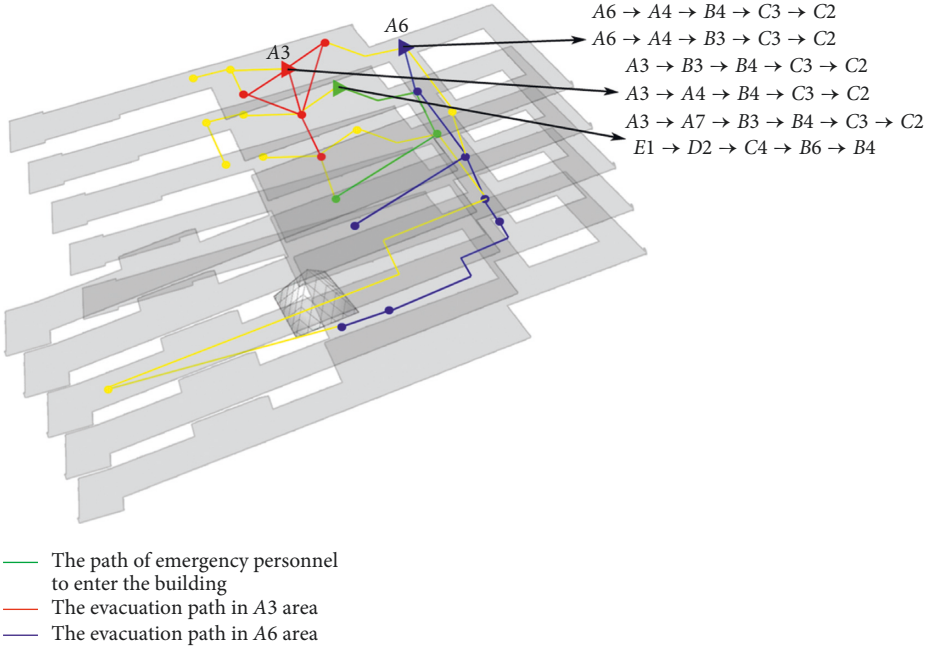

(b)

Figure 12: Evacuation route contrast diagram two: evacuation route map of (a) areas $A3$ and $A6$ without emergency personnel and (b) zones $A3$ and $A6$ without emergency personnel to enter the bulidings.

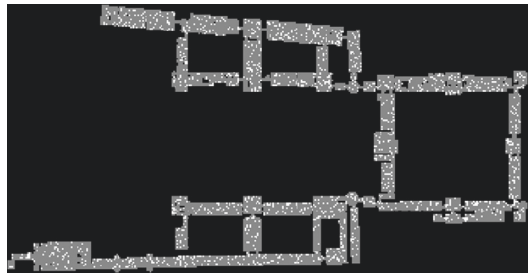

Figure 13: Simulation images of cellular automata on the first floor of the Louvre.

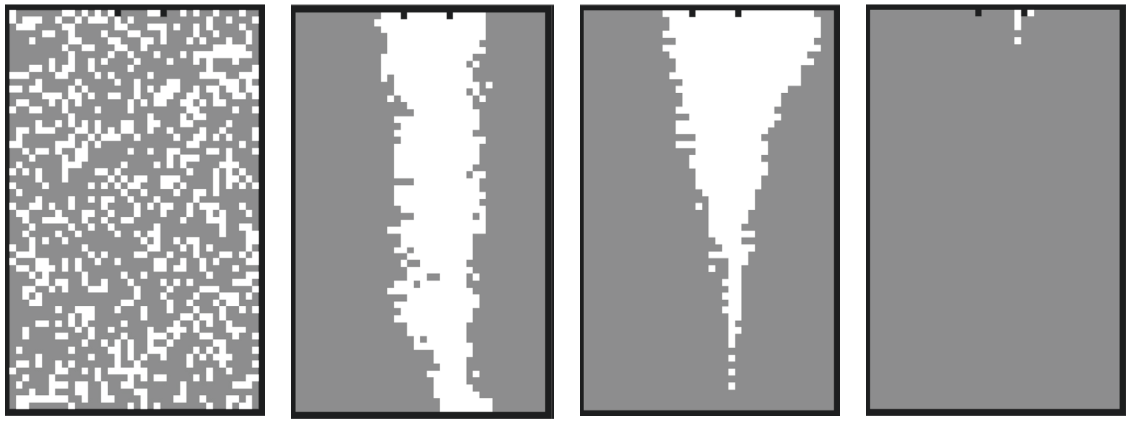

(a) (b) (c) (d)

Figure 14: Simulation diagram of rectangular cellular automata.

Table 5: Simulation results table of L-type channels.

Times of experiments	1	2	3	4	5	6	7	8	9	10
Evacuation time (unit step 0.5 s)	363	350	341	351	376	334	345	339	364	372
Maximum bottleneck area (grid)	340	370	364	397	354	384	364	312	336	387

(a) (b) (c)

Figure 15: Evacuation model diagram of the L-shaped channel spatial structure.

the number of evacuees is 800. The safety exit is located at the center of the wall on the left of the corner, whose size is 8 units. The simulation results are shown in Table 6.

Through ten times of simulation results, the standard deviation of evacuation time was 10.6719, which shows the range of experimental data was small and the simulation was stable. Compared to the rectangular spatial structure, the bottleneck was not easy to occur. The average value of the maximum bottleneck area obtained by simulation was 167.9, as the evacuation results of the L-shaped channel were more stable.

5.1.3. Compound Structure. Figure 16 shows a simulation diagram of a multistructure evacuation model. The evacuation of people in complex terrain was simulated based on

Table 6: Path planning table in a normal emergency.

Number of experiments (times)	1	2	3	4	5	6	7	8	9	10
Evacuation time (unit step 0.5 s)	382	378	391	381	376	394	401	412	384	392
Maximum bottleneck area (grid)	160	210	154	124	154	178	184	162	196	157

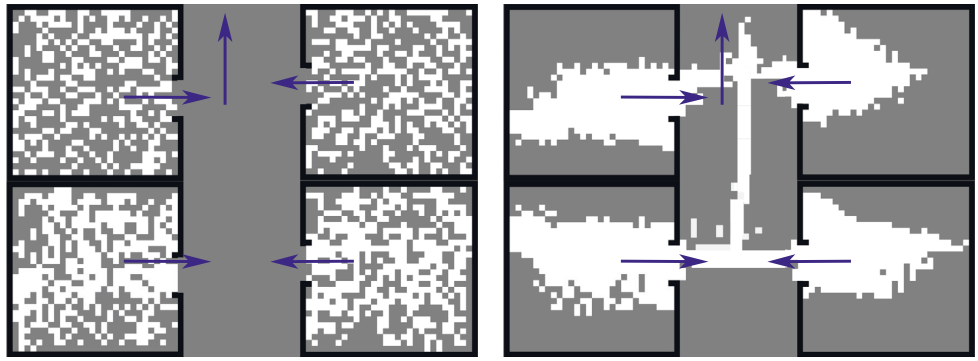

(a) (b)

Figure 16: Evacuation model diagram of the compound structure.

the CA model. Four cellular spaces were all 60×40 rectangular space structure with 400 evacuees in each space. It can be seen that the bottlenecks always occur at the narrower exits, while the main channel was unobstructed.

5.1.4. Stability Analysis. The Grubbs criterion [22] was used to test the stability of the model fitting, which is based on normal distribution and is often used to judge the stability of industrial instrument data. It declares that if the residual V_i of a measured value x_i satisfies the lower formula $|V_i| = |x_i - x| \geq g(n, a) \times \sigma(x)$, the data should be reduced. The experimental data of the rectangular spatial structure evacuation model and the L-channel spatial structure evacuation model in the simulation above were processed and verified.

According to the Grubbs critical value table, when the test data were 11 groups, the average value of evacuation time data is 353.5, and the standard deviation is 13.8076. When the abnormal probability of its data is 95%, $g(n, a) = 2.234$ and residual error $V_i = 30.8462$. The reasonable range of data is (322.6538, 384.3462). Observation and measurement data showed that the simulation data were distributed in the interval and the model output results were stable.

5.2. Influence of Visitor Diversity. The competitiveness of ordinary tourists and disabled tourists in the cellular automata model was different. In the simulation model of this paper, competitiveness discrimination was simply divided into matrices Com $\in \{0, 1\}$. The competitiveness of ordinary tourists was 1, and the competitiveness of disabled tourists was 0. The simulated curves of evacuation time and the proportion of disabled tourists are shown in Figure 17.

It is shown that the evacuation time would increase nonlinearly with the increase in the proportion of tourists of disabilities.

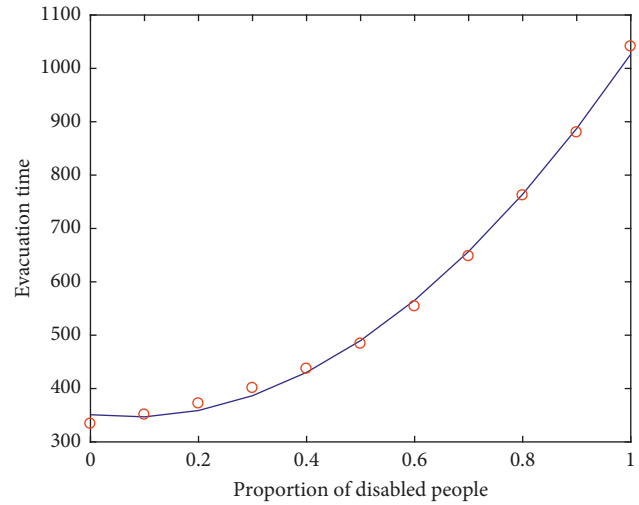

Figure 17: Functional relationship between evacuation time and the ratio of disabled tourists.

For the simulation data, regression analysis was carried out further based on the polynomial regression function $y = a_n \cdot x^n + a_{n-1} \cdot x^{n-1} + \cdots + a_1 \cdot x^1 + a_0$. The quadratic regression analysis by polyfit function of Matlab [17] gave that the polynomial coefficients were 795.3380, 119.7016, and 350.9371.

5.3. Simulation Data Analysis. Based on the model, there may be a functional relationship among the evacuation time T, the pedestrian density, and the exit width L. Simulation is based on the rectangular spatial structure, as shown in Figure 18. The main channel grids $L_E = 10$, and the number of evacuees was 880, 960, 1024, respectively. The size of the cellular space was 60×40, and the number of simulated evacuees was 800. The functional images are shown in Figure 19. The functional relationship of evacuation time and pedestrian density at different exit widths was as follows.

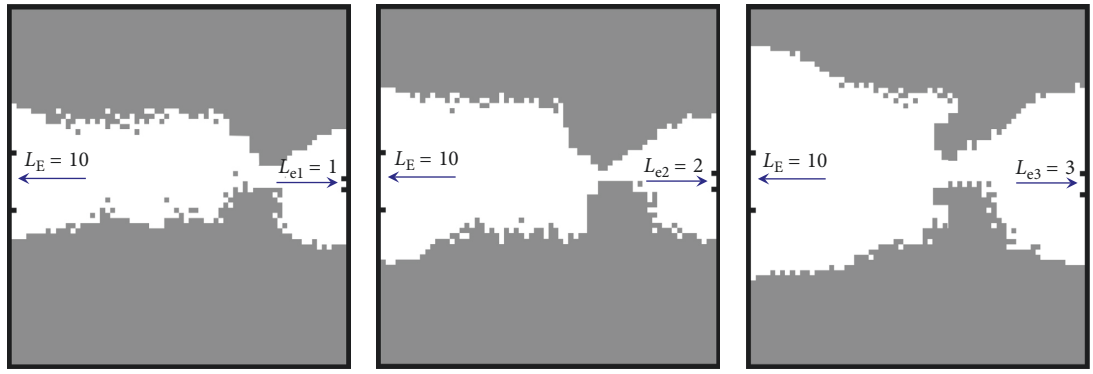

Figure 18: Evacuation model diagram of a rectangular spatial structure: (a) $L_{e1} = 1$; (b) $L_{e2} = 2$; (c) $L_{e3} = 3$.

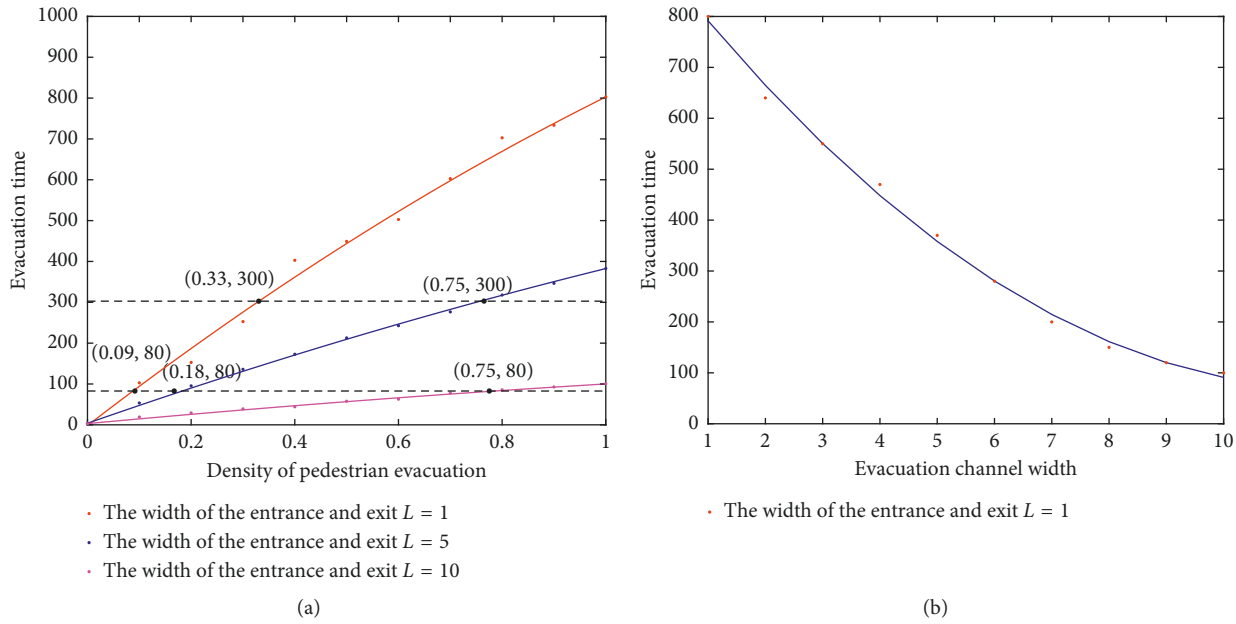

Figure 19: Functional relationship between evacuation time and pedestrian density at different exit widths.

Line $L = 1$: $y_{l=1} = 819.09x + 16.82$; fitting curve's correlation coefficient $R^2 = 0.990 > 0.950$. It is considered that the fitting curve has good correlation.

Line $L = 5$: $y_{l=5} = 364.09x + 19.77$. Fitting line $L = 1$: $y_{l=1} = 819.09x + 16.82$; fitting curve's correlation coefficient $R^2 = 0.990 > 0.950$. It is considered that the fitting curve has good correlation.

Line $L = 10$: $y_{l=10} = 92.18x + 8.09$; fitting curve's correlation coefficient $R^2 = 0.986 > 0.950$. It is considered that the fitting curve has good correlation.

The theoretical analysis showed that the evacuation time tends to infinity when the channel length is 0, and the evacuation time was larger than zero when the channel length tends to infinity. Hence, the relationship among the functions should be an inverse proportional function. Assume that the function relation was $y = (a/(x + b)) + c$. Through the nonlinear fitting by function Nlinfit of Matlab [17], the simulation results of the function were given as follows.

$$y = \frac{14644}{(x + 8.7405)} - 705.4753. \tag{10}$$

The function relation with egress time T, outlet width L, and population density to be evacuated ρ was shown as follows:

$$S_{ij} = T = g^S(L, \rho) = k \cdot \rho + b = \frac{a}{L + b} + c. \tag{11}$$

6. Conclusion

This paper proposed a novel evacuation model instruction. Main contributions are as follows. First, the evaluation formula was proposed to analyse the patency of the buildings. The routes on the images of each floor in the buildings can be directly shown by three-dimensional architectural model after obtaining the binary image of the active region in a multistory building. The multistory

building evacuation algorithm was established to provide the schemes of optimal evacuation routes. The result of evacuation routes in different emergency situations was discussed and compared in this paper. Simulation in CA illustrated the efficiency of the model that the stability and reliability of the simulation results were verified by Grubbs criterion. Then, different factors were considered, such as diversity of tourists, pedestrian density, and width of exit. Furthermore, a functional relationship was clearly given among the evacuation time with those factors, and the functional relationship has a good correlation. It was applied to optimize the initial evacuation routes. Based on these, the algorithm can adapt to different circumstances, and an accurate time of leaving the buildings can be calculated accurately.

Data Availability

No data were used to support this study.

Conflicts of Interest

The authors declare that there are no conflicts of interest regarding the publication of this paper.

Authors' Contributions

YZ planned the study. YZ and ZF performed the research. YZ wrote the first manuscript. YZ, TW, GZ, and ZF read and approved the final manuscript.

Acknowledgments

The authors wish to express their gratitude for the financial support from Fundamental Research Funds for the Central Universities (no. XDJK2019C035).

References

[1] J. Tavares, "The open society assesses its enemies: shocks, disasters and terrorist attacks," *Journal of Monetary Economics*, vol. 51, no. 5, pp. 1039–1070, 2004.

[2] N. Amoretti, "Terrorist attack in nice, France, in July 2016: massive influx of patients to a radiology department," *Radiology*, vol. 288, no. 1, pp. 2-3, 2018.

[3] S. Galea, J. Ahern, H. Resnick et al., "Psychological sequelae of the September 11 terrorist attacks in New York city," *New England Journal of Medicine*, vol. 346, no. 13, pp. 982–987, 2002.

[4] J. Ahern, S. Galea, H. Resnick et al., "Television images and psychological symptoms after the September 11 terrorist attacks," *Psychiatry: Interpersonal and Biological Processes*, vol. 65, no. 4, pp. 289–300, 2002.

[5] Telegraph Media Group, *Terror Attacks in France: from Toulouse to the Louvre*, Telegraph Media Group, London, UK, 2018, http://www.telegraph.co.uk/news/0/terror-attacks-france-toulouse-louvre/.

[6] 8.1 Million Visitors to the Louvre in 2017, Louvre Press Release, January 2018, presse.louvre.fr/8-1-million-visitors-to-the-louvre-in-2017/.

[7] N. Pelechano and A. Malkawi, "Evacuation simulation models: challenges in modeling high rise building evacuation with cellular automata approaches," *Automation in Construction*, vol. 17, no. 4, pp. 377–385, 2008.

[8] X. Zheng, T. Zhong, and M. Liu, "Modeling crowd evacuation of a building based on seven methodological approaches," *Building and Environment*, vol. 44, no. 3, pp. 437–445, 2009.

[9] P. A. Thompson and E. W. Marchant, "A computer model for the evacuation of large building populations," *Fire Safety Journal*, vol. 24, no. 2, pp. 131–148, 1995.

[10] J. M. Smith, "State-dependent queueing models in emergency evacuation networks," *Transportation Research Part B: Methodological*, vol. 25, no. 6, pp. 373–389, 1991.

[11] J. Pauls, "Calculating evacuation times for tall buildings," *Fire Safety Journal*, vol. 12, no. 3, pp. 213–236, 1987.

[12] Y. Liu, N. Okada, D. Shen, and S. Li, "Agent-based flood evacuation simulation of life-threatening conditions using vitae system model," *Journal of Natural Disaster Science*, vol. 31, no. 2, pp. 69–77, 2009.

[13] J. Ma, S. M. Lo, and W. G. Song, "Cellular automaton modeling approach for optimum ultra high-rise building evacuation design," *Fire Safety Journal*, vol. 54, pp. 57–66, 2012.

[14] L. Zhang, Y. Wang, H. Shi, and L. Zhang, "Modeling and analyzing 3D complex building interiors for effective evacuation simulations," *Fire Safety Journal*, vol. 53, pp. 1–12, 2012.

[15] Q. Xiong, Q. Zhu, Z. Du et al., "A dynamic indoor field model for emergency evacuation simulation," *ISPRS International Journal of Geo-Information*, vol. 6, no. 4, p. 104, 2017.

[16] J. Sauvola, T. Seppanen, S. Haapakoski, and M. Pietikainen, "Adaptive document binarization," in *Proceedings of the Fourth International Conference on Document Analysis and Recognition*, vol. 1, IEEE, Ulm, Germany, August 1997.

[17] S. Si, *Mathematical Modeling Algorithm and Application Problem Solving*, National Defense Industry Press, Beijing, China, 2011.

[18] E. Diday and J. C. Simon, "Clustering analysis," in *Digital Pattern Recognition*, Springer, Berlin, Heidelberg, 1976.

[19] H. Yue, C.-F. Shao, and Z.-S. Yao, "Pedestrian evacuation flow simulation based on cellular automata," *Acta Physica Sinica*, vol. 58, no. 7, pp. 4523–4530, 2009.

[20] V. C. Rideout, *Mathematical and Computer Modeling of Physiological Systems*, Prentice Hall, Upper Saddle River, NJ, USA, 1991.

[21] X.-H. Cui, Q. Li, J. Chen, and C.-X. Chen, "Study on occupant evacuation model in large public place: to consider individual character and following behavior," *Ziran Zaihai Xuebao/Journal of Natural Disasters*, vol. 14, no. 6, pp. 133–140, 2005.

[22] F. E. Grubbs, "Sample criteria for testing outlying observations," *Annals of Mathematical Statistics*, vol. 21, no. 1, pp. 27–58, 1950.